

The use of crista galli morphology and morphometry in sex determination: a cone-beam computed tomography study

Ö. Okumuş

Department of Dentomaxillofacial Radiology, Faculty of Dentistry, Altınbaş University, İstanbul, Turkey

[Received: 3 June 2022; Accepted: 16 August 2022; Early publication date: 25 August 2021]

Background: The morphology of crista galli (CG) varies from one individual to another and its structure may be pneumatized or compact bone. This study purposed to investigate the morphometry of the CG on cone-beam computed tomography (CBCT) scans, to apply morphological classification based on the characteristics of the CG morphometry and to analyse the association of morphological and morphometric features with sex.

Materials and methods: The width, length, and height of the CG were calculated on the CBCT scans of 400 patients (233 females, 167 males). The CG was categorised into three morphological types and the presence of the CG pneumatization and the Keros classification were examined.

Results: The average length of the CG was 12.93 ± 2.12 mm, the average width of CG was 4.79 ± 1.54 mm, and the average height of CG was 16.21 ± 2.73 . There was no statistical difference between sexes in both height and length values. The mean CG width of female patients was found to be statistically significantly higher than that of male patients. No statistically significant difference was determined between the morphological types of CG and sex. For width only, the area under the receiver-operating characteristic curve was found to be significantly higher than 0.5 and the cutoff value for the width parameter was determined as 4 mm.

Conclusions: The morphologic and morphometric features of CG, presence of pneumatization and relation of the anatomy of olfactory region to CG can be analysed in detail using CBCT. The mean CG width of female patients was found significantly higher than that of male patients. However, further studies with different populations and modalities are needed to evaluate the relationship between morphologic and morphometric features of CG and sex. (Folia Morphol 2022; 81, 4: 1005–1013)

Key words: cone-beam computed tomography, crista galli, olfactory fossa, morphology, pneumatization, sex determination

INTRODUCTION

The crista galli (CG) is an anatomical landmark that is located in the midline above the cribriform plate

of the ethmoid bone. It is a smooth, thick, triangular bony process and appears as a ridge in the anterior part of the anterior cranial fossa. The thin and long

Address for correspondence: Dr. Ö. Okumuş, Altınbaş University, Faculty of Dentistry, Department of Dentomaxillofacial Radiology, Zuhuratbaba, İncirli Street, No: 11, Bakırköy, İstanbul, 34147 Turkey, e-mail: dtozlemsen@hotmail.com

This article is available in open access under Creative Common Attribution-Non-Commercial-No Derivatives 4.0 International (CC BY-NC-ND 4.0) license, allowing to download articles and share them with others as long as they credit the authors and the publisher, but without permission to change them in any way or use them commercially.

posterior margin of the CG serves for the attachment of the falx cerebri. The thick and short anterior margin articulates with the frontal bone. To complete the foramen cecum, it has two small projecting alae, which are received into corresponding depressions in the frontal bone [3, 8, 20, 30]. In addition, CG is an endoscopic surgical landmark in pituitary surgery and frontal sinus approach [8]. In some individuals it can also be pneumatized, although the CG is usually a compact bony structure [32].

In forensic and archaeological examinations, sex determination is an important parameter that helps to establish the biological profile of the deceased [6]. Two types of helpful procedures for sex determination are present: morphometric and morphological. Morphometric analysis includes statistical analysis and comparison of measurements to develop a probabilistic estimation of sex, while morphological analysis is subjective and includes the visual examination of dimorphic traits [16, 33].

Sex assessment by examining the dimorphism of the pelvic bone and skull has been reported to have the highest accuracy and has been found to be extremely useful in forensic science [16, 33]. Knowledge of the sex characteristics of small parts of the skeleton is of great importance for sex determination in cases where bone integrity is not preserved [2].

Various radiological imaging modalities especially computed tomography (CT) are used to estimate sex from the cranial parameters [23]. CT has become the most preferred modality for sex estimation because it can display complex bone structures in detail and thus reliable morphometric measurements can be provided [28]. Recently, cone-beam computed tomography (CBCT) has become an alternative imaging modality to CT for the examination of skull anatomy as it supplies higher resolution images with isometric voxel, low radiation dose, and lower costs [9].

The morphology of CG varies from one individual to another and its structure may be pneumatized or compact bone. It was purposed to investigate the morphometric characteristics of CG in CBCT scans and to evaluate the association of morphological and morphometric features of CG with sex in the Turkish population.

MATERIALS AND METHODS

This retrospective study was approved by the Clinical Research Ethical Committee of Altınbaş University (approval number: 2022/114). The study group

consisted of the records of the patients in the CBCT archive of Altınbaş University, Faculty of Dentistry, Department of Dentomaxillofacial Radiology, Istanbul, Turkey. Before CBCT examinations, patients routinely sign written consent forms.

Individuals with any history of surgery or trauma affecting the CG structure and poor quality images were excluded. Patients over 18 years and whose images showed the medium and superior parts of the face for the examination of the crista galli of the ethmoid bone and the nasal fossa were included in the study. The study sample consisted of CBCT scans of 400 patients (233 females and 167 males) between the ages of 18 and 87 years with a mean age of 44.10 ± 16.90 .

Cone-beam computed tomography images of all patients were acquired with NewTom VGi EVO (CeflaGroup, Verona, Italy). The device was set for 1–32 mA and 110 kV with a single 360 degree rotation created images with a voxel size of 0.3 mm. NNT Viewer software (CeflaGroup, Verona, Italy) was used for measurements and the images were in a quiet, dark room on a 22" high image quality Barco medical monitor (Barco, Kortrijk, Belgium) to provide an effective evaluation for CBCT.

The width, height and length of the CG were calculated and based on the morphometric features of the CG, the morphological classification was performed. In addition, the presence of the CG pneumatization was evaluated on CBCT image and the Keros classification [14, 16] was conducted.

Image analysis

Crista galli dimensions

The height of the CG on coronal view, the width and length of the CG on axial view were measured. On coronal view, the highest point between the cribriform plate and the CG was calculated as the height of CG (Fig. 1). On axial view, the greatest transverse measurement of the CG with reference of the outer cortical borders of the CG was calculated as the width CG (Fig. 2). On axial view, the greatest anteroposterior diameter of the CG from the end of the inner cortex of frontal bone was recorded as the length (Fig. 3).

Classification of morphology

The CG size measurements and the cavitory component presence were the main criteria for morphological classification. According to this classification [16]:

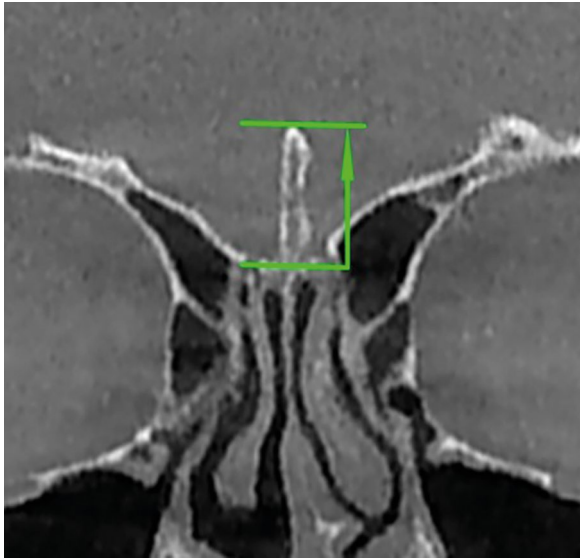


Figure 1. Measurement of the height of the crista galli on coronal cone-beam computed tomography image.

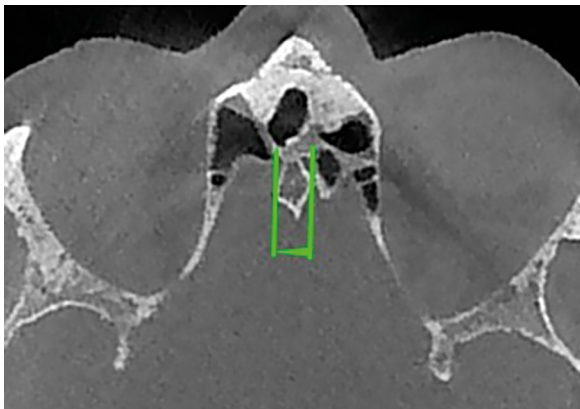


Figure 2. Measurement of the width of the crista galli on axial cone-beam computed tomography image.

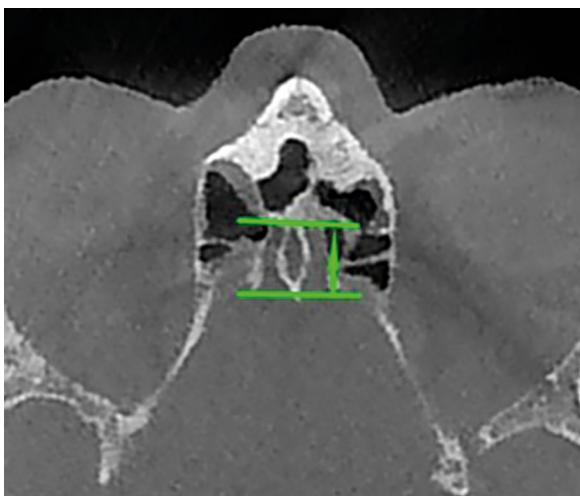


Figure 3. Measurement of the length of the crista galli on axial cone-beam computed tomography image.

- type I (teardrop type): the width of CG greater than one-third of its height, and containing a wide cavitory component (Fig. 4A);
- type II (tubular type): the width of CG less than one-third of its height and including a cavitory component from the base to the apex (Fig. 4B);
- type III (ossified type): the width of CG less than one-third of its height but did not contain a cavitory component (Fig. 4C).

Classification of Keros

The depth of olfactory fossa was classified into three categories according to the height of the lateral lamella of the cribriform plate by Keros [14]. It is the classical technique generally used in studies regarding the olfactory region anatomy and the CG [16, 22].

The Keros classification divides the depth of olfactory fossa into three categories according to the lateral lamellae of the cribriform plate [14]. According to this classification:

- type 1: height between 1 and 3 mm. The lateral lamella is short and the ethmoid roof is approximately the same plane as the cribriform plate (Fig. 5A);
- type 2: height between 4 and 7 mm. The lateral lamella is longer (Fig. 5B);
- type 3: height between 8 and 16 mm. The ethmoid roof is clearly above the cribriform plate (Fig. 5C).

Assessment of presence of CG pneumatization

The presence of CG pneumatization was evaluated on the coronal view (Fig. 6).

Statistical analysis

For all statistical analyses, SPSS Statistics 22 (SPSS IBM, Turkey) software program was used. To compare the normally distributed parameters between two groups, Student's t test was used. To compare qualitative data, Yates Continuity Correction and Chi-square test were used. The most appropriate cut-off points were selected according to the receiver-operating characteristic (ROC) analysis. P values < 0.05 were considered as statistically significant.

RESULTS

This study was carried out on 400 cases, 167 (41.8%) male and 233 (58.1%) female between 18 and 87 years old and the mean age of all individuals was 44.10 ± 16.90 . The mean age of female patients was 42.36 ± 16.51 years (18–87 years), while the

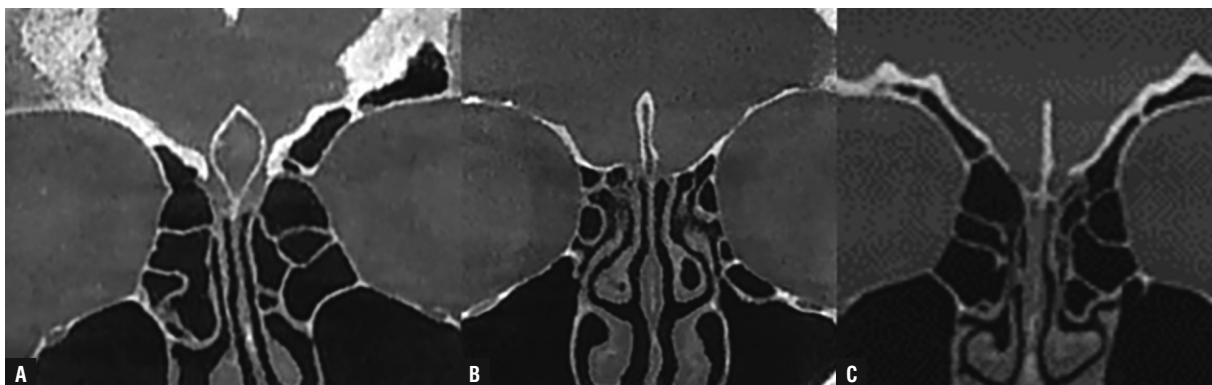


Figure 4. Morphological classification of crista galli on coronal cone-beam computed tomography images; **A.** Teardrop type; **B.** Tubular type; **C.** Ossified type.

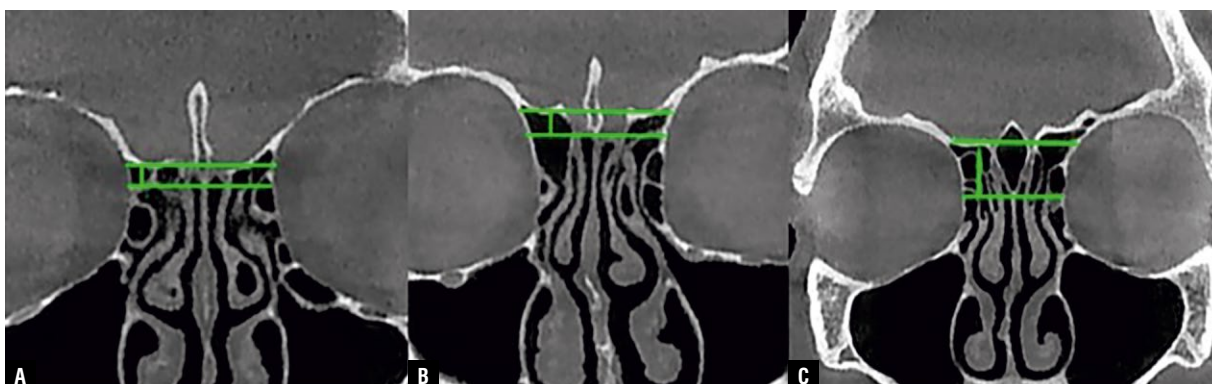


Figure 5. Keros classification on coronal cone-beam computed tomography images; **A.** Keros type 1; **B.** Keros type 2; **C.** Keros type 3.

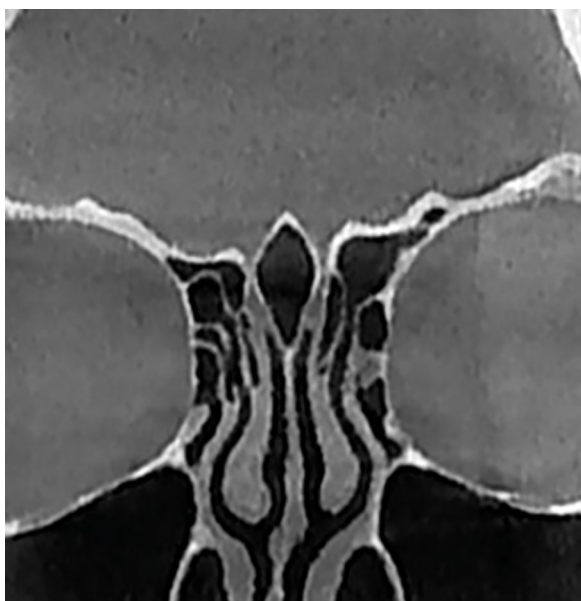


Figure 6. A pneumatized crista galli on coronal cone-beam computed tomography image.

mean age of male patients was 46.54 ± 17.18 years (18–85 years).

The average length of the CG was 12.93 mm, the average width of CG was 4.79 mm, and the average height of CG was 16.21 mm (Table 1). There was no statistical difference between sex and both height and length values ($p > 0.05$). The mean CG width of female patients was found significantly higher than that of male patients ($p = 0.013$) (Fig. 7).

Among the cases, regarding the morphological classification, 184 (46%) were classified as type I, 202 (50.5%) were type II, and 14 (3.5%) were type III (Table 2). No statistically significant relationship was determined between the morphological types of CG and sex ($p > 0.05$).

Regarding the Keros classification, 78 (19.5%) cases were classified as type I, 176 (44%) were type II, and 146 (36.5%) were type III (Table 3). There was a statistically significant difference between sexes in respect of Keros classification ($p < 0.05$).

Table 1. Morphometric measurements of the crista galli

	Female		Male		Total		P
	Min–Max	Mean ± SD	Min–Max	Mean ± SD	Min–Max	Mean ± SD	
Height	10.3–25.2	16.35 ± 2.7	10.2–23.7	16.01 ± 2.78	10.2–25.2	16.21 ± 2.73	0.254
Length	5.1–21	12.97 ± 2.02	8.2–20.7	12.87 ± 2.27	5.1–21	12.93 ± 2.12	0.321
Width	2.1–14.8	4.97 ± 1.59	1.5–8.1	4.53 ± 1.43	1.5–14.8	4.79 ± 1.54	0.013*

Student t test, *p < 0.05; Min — minimum; Max — maximum; SD — standard deviation

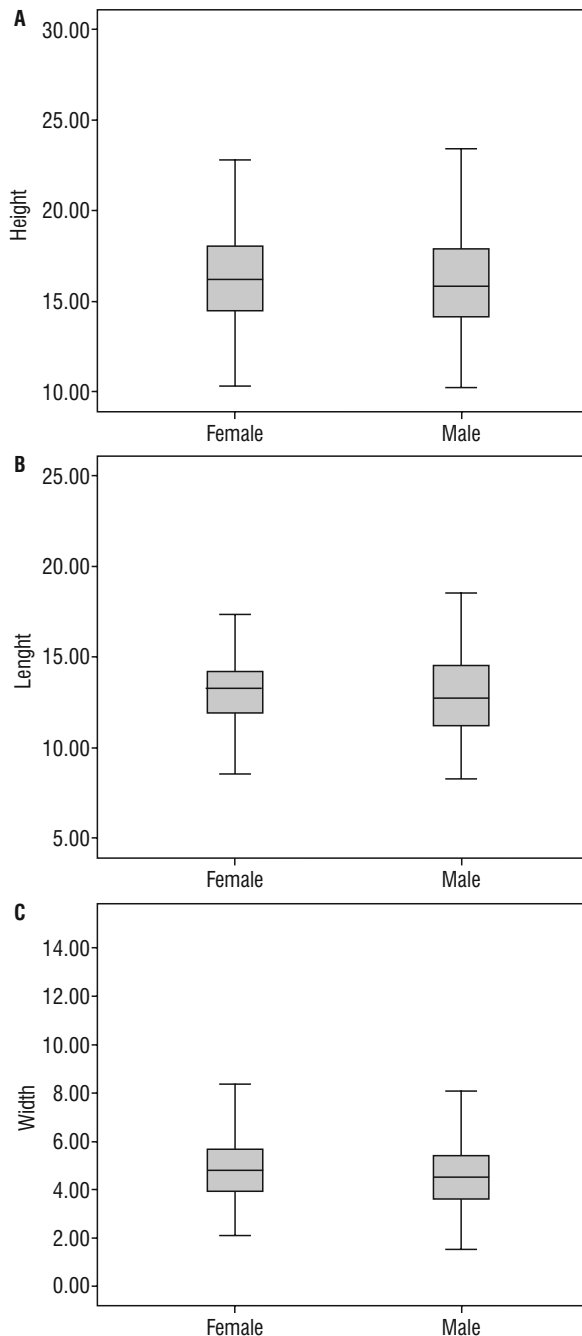


Figure 7. Box plots for height (A), length (B), and width (C) measurements of crista galli regarding sex.

Pneumatization of CG was determined in 42 (10.5%) of the 400 patients, in 15 (9%) males and 27 (11.6%) females (Table 2). No statistically significant difference was found between presence of pneumatization and sex ($p > 0.05$).

Receiver operating characteristic curves were drawn for height, length and width measurements for sex determination (Fig. 8). For width only, the area under the ROC curve was found to be significantly higher than 0.5 ($p < 0.05$). The evaluation of the CG length, height, and width values in sex determination are showed by the ROC analysis results (Table 3). For the width parameter, the cut-off value was found as 4 mm, and this value demonstrated 73.4% specificity for female sex differentiation and 41.9% sensitivity for male sex differentiation. Since the areas under the curve for height and length were not significantly higher than 0.5, the cut-off point could not be calculated ($p > 0.05$).

DISCUSSION

The CG is located in the midline above the cribriform plate and derives from the ethmoid bone. Embryologically, during the second foetal month, it is formed by mesethmoidal cartilage together with the perpendicular plate of the ethmoid bone and the central structures of the anterior skull base [20]. CG ossification usually starts at the second postnatal month, steadily increases until the 14th month, afterwards slowly progresses the 24th month [15].

Sex determination is one of the most essential procedures in forensic examination [23]. Studies have shown that the cranium is the next best contributor to sex assessment after the pelvis. Krogman and Iscan [18] have reported that sex can be determined from the pelvis with an accuracy of 95% and from the cranium with an accuracy of 92%. Cranium investigations are based on morphometric analyses, and accuracy rates have been investigated in different populations [17, 21, 26]. Osteometric measurements made

Table 2. The distribution of the morphological and Keros classification and pneumatization status of the crista galli according to sex

	Female, n (%)	Male, n (%)	Total, n (%)	P
Morphological classification:				0.815
Type I	108 (46.4%)	76 (45.5%)	184 (46%)	
Type II	118 (50.6%)	84 (50.3%)	202 (50.5%)	
Type III	7 (3%)	7 (4.2%)	14 (3.5%)	
Keros classification:				0.017*
Type I	38 (16.3%)	40 (24%)	78 (19.5%)	
Type II	116 (49.8%)	60 (35.9%)	176 (44%)	
Type III	79 (33.9%)	67 (40.1%)	146 (36.5%)	
Pneumatization status:				0.501 ⁺
Present	27 (11.6%)	15 (9%)	42 (10.5%)	
Absent	206 (88.4%)	152 (91%)	358 (89.5%)	

Chi-square test, *Yates Continuity Correction, ⁺p < 0.05**Table 3.** Receiver operating characteristic analysis results in sex determination of crista galli width, height, and length values

	Height	Length	Width
AUC (95% CI)	0.533 (0.483–0.583)	0.529 (0.479–0.579)	0.572 (0.522–0.621)
P value	0.257 (p > 0.05)	0.335 (p > 0.05)	0.014* (p < 0.05)
Cut-off value (for male)	–	–	≤ 4
Cut-off value (for female)	–	–	> 4
Sensitivity (%) (male)	–	–	41.9
Specificity (%) (female)	–	–	73.4

AUC — area under curve; CI — confidence interval

using radiological methods have many advantages, such as being non-bone-destructuring methods, not requiring cleaning of the bones, and being more practical and applicable than many other methods [11]. Advanced radiological methods, such as CBCT, multi-slice CT imaging are important for osteometric measurements. The CG can be easily examined morphometrically and morphologically on CBCT images. In addition, during embryological process, the differences in the ossification rate and termination period of ossification of CG may be related to sex features [16].

In the literature, there are a few studies examining the morphometry of CG. In a study conducted on CT images of 196 patients, the dimensions of pneumatized CG were examined. There was no statistically significant relationship between CG anteroposterior diameter and sex, the CG craniocaudal diameter was slightly longer in males than females and a significant relationship was found in the latero-lateral diameter of CG in males and females [19].

In another study, Mladina et al. [20] declared that the pneumatized CG height was significantly higher in females than in males on CBCT images of 102 skulls. In another retrospective study with CBCT images of 300 subjects, performed by Uçar et al. [32], the average width and length dimensions of the CG were reported to be 14.05 ± 2.98 and 3.69 ± 1.53 mm, respectively, in males, and 14.02 ± 2.90 and 3.77 ± 1.43 mm in females. No significant difference was found between the length and width dimensions of CG and sex. In a recent study of the CT images of 533 patients, Komut and Golpınar [16] found a statistically significant relationship between sex and CG measurements and reported the length, height, and width measurements of CG can be used in the sex determination. In the current study, the average CG height, length, and width values were 16.01 ± 2.78 , 12.87 ± 2.27 , and 4.53 ± 1.43 mm, respectively in males, and 16.35 ± 2.7 , 12.97 ± 2.02 , and 4.97 ± 1.59 mm, respectively, in females. There was no statistical difference between sexes in height and

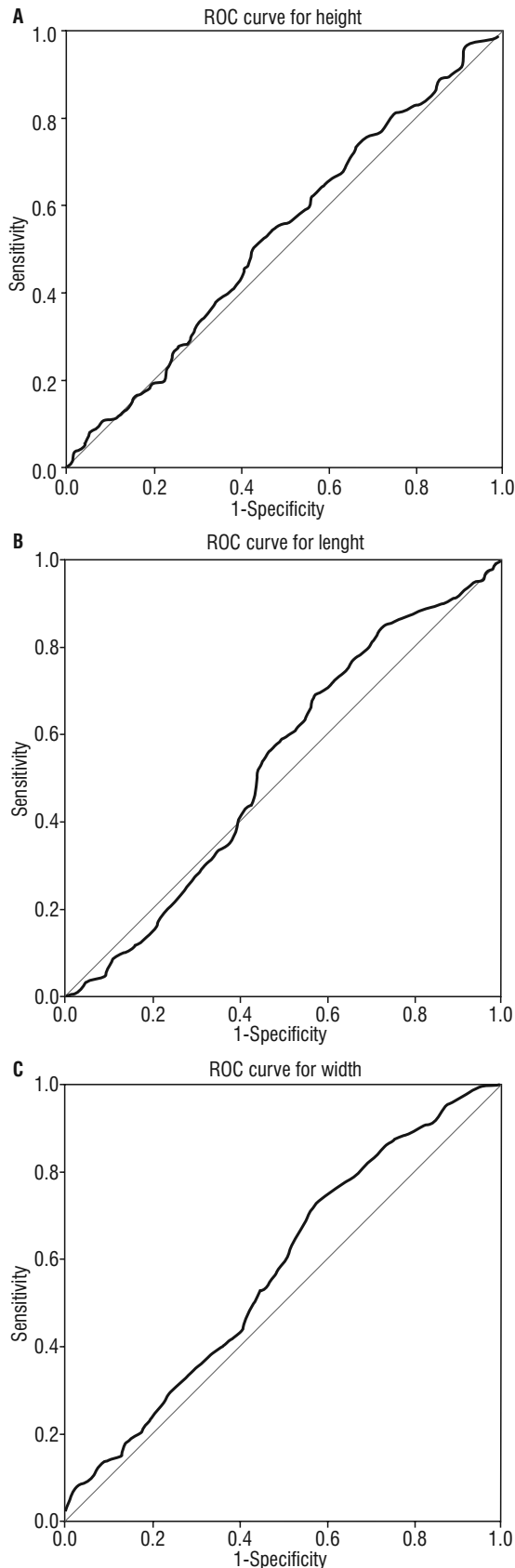


Figure 8. Receiver operating characteristic (ROC) curves showing the predictive power of height (A), length (B), and width (C) measurements of crista galli in sex discrimination.

length values but the mean CG width of females was found significantly higher than that of males (Table 4).

Furthermore, Komut and Golpınar [16] examined the classification of morphology with objective criteria of radiology. They reported that there was a statistically significant relationship between the new morphological types of CG and sex, and that this classification could be used for sex determination. In contrast to this study, in our study, 184 (46%) were classified as teardrop type, 202 (50.5%) were tubular type, and 14 (3.5%) were ossified type. No statistically significant difference was determined between the morphological types of CG and sex.

The Keros classification divides the depth of olfactory fossa into three categories according to the lateral lamellae of the ciribriform plate [14]. It is the classical modality generally used in studies of CG and the anatomy of olfactory region [22]. In a study evaluating CT images, 178 (81.6%) were classified as Keros I, 39 (17.9%) were Keros II, and 1 (0.5%) were Keros III and there was a significant difference between males and females [22]. In another CBCT study of 174 patients, the most common Keros classification was type II (65.52%), followed by type III (20.69%) and type I (13.79%) and no significant relation between sex and Keros types was reported [9]. In another study, Mladina et al. [20] declared that type I has been found in 29 cases (42.64%), type II has been found in 38 cases (55.88%), and type C in 1 case (1.47%) on CBCT images of 102 skulls. In a study conducted on CT images of 150 subjects, there was a significant difference in respect of the distribution of Keros type II between males and females [4]. In a recent study by Komut and Golpınar [16], of the CT images of 533 patients, Keros type I was found to be 52% and 48%, respectively in males and females; Keros type II was found to be 51.7% and 48.3%; Keros type III was found to be 40.9% and 59.1% and no statistically significant difference was reported between sex and Keros types. In the current study, the most prevalent Keros classification was type II (44%) followed by type III (36.5%) and type I (19.5%). There was a statistically significant difference between sexes in respect of Keros classification.

In the literature, the incidence of pneumatization of CG was examined in the vast majority of the previous studies [1, 3, 5, 6, 8, 10, 13, 16, 19, 20, 24, 25, 29, 30–32]. The incidence of pneumatization of the CG was in a wide range (2.3% to 66.6%) [16, 20]. In this study, pneumatization of CG was determined in

Table 4. The mean values of crista galli in previous studies

Previous studies	Population	Mean height [mm]	Mean length [mm]	Mean width [mm]	Method
Kim et al. [14]	Korea	17.98 ± 3.7	–	–	CT
Manea & Mladina [20]	Romania	5.0–14.8	4.7–12.7	3.0–6.8	CT
Mladina et al. [4]	Croatia	10.1 ± 3.0	7.1 ± 2.5	3.0 ± 1.2	Skull-CBCT
Uçar et al. [5]	Turkey	–	14.03 ± 2.93	3.73 ± 1.48	CBCT
Komut & Gulpinar [7]	Turkey	14.22 ± 3.11	12.78 ± 2.50	3.57 ± 1.48	CT

CT — computed tomography; CBCT — cone-beam computed tomography

Table 5. The incidence of pneumatization of crista galli in previous studies

Previous studies	Population	Incidence (%)	Method
Bašić et al. [26]	Croatia	2.4	CT
Som et al. [23]	USA	13	CT
Al-Qudah [25]	Jordan	28	CT
Hajjioannou et al. [28]	UK	14.1	CT
Kim et al. [14]	Korea	12.2	CT
Cobzeanu et al. [3]	Romania	22.92	CT
Poje et al. [29]	Croatia	37.5	CT
Manea & Mladina [20]	Romania	30.1	CT
Tetiker et al. [2]	Turkey	21	CT
Çalışkan et al. [27]	Turkey	5	CBCT
Mladina et al. [4]	Croatia	66.6	Skull/CBCT
Şahan et al. [24]	Turkey	16	CT
Thai et al. [30]	USA	3.8	CBCT
Akiyama & Kondo [1]	Japan	9.3	CT
Acar et al. [22]	Turkey	29.8	CT
Komut & Gulpinar [7]	Turkey	2.3	CT
Uçar et al. [5]	Turkey	17.67	CBCT

CT — computed tomography; CBCT — cone-beam computed tomography

42 (10.5%) of the 400 patients and no statistically significant difference was found between presence of pneumatization and sex. Consistent with the current study, a few previous studies reported no relation between sex and pneumatization [1, 15, 16]. In contrast, Çalışkan et al. [10] reported a relationship between sex and pneumatization of CG (Table 5).

In the literature, there are several studies regarding sex determination using different anatomical structures in the cranium [7, 12, 27]. Besides, there is only one study regarding the association between the morphological and morphometric features of CG and sex [16]. In the current study, there was no statistical difference in height and length values between sex, but the mean CG width of females was found significantly higher than that of males. Therefore,

further studies with different populations and modalities with a greater number of subjects are needed to evaluate the relationship between morphologic and morphometric features of CG and sex and also age to confirm the findings.

CONCLUSIONS

In conclusion, based on CBCT imaging results: (i) No statistically significant difference was determined between the morphological types of CG and sex; (ii) A statistically significant difference between sexes in respect of Keros classification was found; (iii) No statistically significant difference was found between presence of pneumatization and sex; (iv) No statistical relationship between sex and height and length values was determined, but the mean CG width of females was found significantly higher than that of males; (v) The morphologic and morphometric features of CG, presence of pneumatization and relation of the anatomy of olfactory region to CG can be analysed in detail using CBCT.

Conflict of interest: None declared

REFERENCES

1. Acar G, Cicekcibasi AE, Koplay M, et al. The relationship between the pneumatization patterns of the frontal sinus, crista galli and nasal septum: a tomography study. *Turk Neurosurg.* 2020; 30(4): 532–541, doi: [10.5137/1019-5149.JTN.26006-19.4](https://doi.org/10.5137/1019-5149.JTN.26006-19.4), indexed in Pubmed: [31736030](https://pubmed.ncbi.nlm.nih.gov/31736030/).
2. Akhlaghi M, Bakhtavar K, Moarefdoost J, et al. Frontal sinus parameters in computed tomography and sex determination. *Leg Med (Tokyo).* 2016; 19: 22–27, doi: [10.1016/j.legalmed.2016.01.008](https://doi.org/10.1016/j.legalmed.2016.01.008), indexed in Pubmed: [26980249](https://pubmed.ncbi.nlm.nih.gov/26980249/).
3. Akiyama O, Kondo A. Classification of crista galli pneumatization and clinical considerations for anterior skull base surgery. *J Clin Neurosci.* 2020; 82(Pt B): 225–230, doi: [10.1016/j.jocn.2020.11.005](https://doi.org/10.1016/j.jocn.2020.11.005), indexed in Pubmed: [33246906](https://pubmed.ncbi.nlm.nih.gov/33246906/).
4. Alazzawi S, Omar R, Rahmat K, et al. Radiological analysis of the ethmoid roof in the Malaysian population. *Auris Nasus Larynx.* 2012; 39(4): 393–396, doi: [10.1016/j.anl.2011.10.002](https://doi.org/10.1016/j.anl.2011.10.002), indexed in Pubmed: [22055509](https://pubmed.ncbi.nlm.nih.gov/22055509/).

5. Al-Qudah MA. Anatomical variations in sino-nasal region: a computer tomography (CT) study. *J Med J.* 2010; 44: 290–297.
6. Basić N, Basić V, Jukić T, et al. Computed tomographic imaging to determine the frequency of anatomical variations in pneumatization of the ethmoid bone. *Eur Arch Otorhinolaryngol.* 1999; 256(2): 69–71, doi: [10.1007/s004050050118](https://doi.org/10.1007/s004050050118), indexed in Pubmed: [10068893](https://pubmed.ncbi.nlm.nih.gov/10068893/).
7. Cekdemir YE, Mutlu U, Karaman G, et al. Estimation of sex using morphometric measurements performed on cranial computerized tomography scans. *Radiol Med.* 2021; 126(2): 306–315, doi: [10.1007/s11547-020-01233-8](https://doi.org/10.1007/s11547-020-01233-8), indexed in Pubmed: [32533549](https://pubmed.ncbi.nlm.nih.gov/32533549/).
8. Cobzeanu MD, Bâldea V, Bâldea MC, et al. The anatomo-radiological study of unusual extrasinusual pneumatizations: superior and supreme turbinate, crista galli process, uncinata process. *Rom J Morphol Embryol.* 2014; 55(3 Suppl): 1099–1104, indexed in Pubmed: [25607391](https://pubmed.ncbi.nlm.nih.gov/25607391/).
9. Costa AL, Paixão AK, Gonçalves BC, et al. Cone beam computed tomography-based anatomical assessment of the olfactory fossa. *Int J Dent.* 2019; 2019: 4134260, doi: [10.1155/2019/4134260](https://doi.org/10.1155/2019/4134260), indexed in Pubmed: [31073308](https://pubmed.ncbi.nlm.nih.gov/31073308/).
10. Çalışkan A, Sumer A, Bulut E. Evaluation of anatomical variations of the nasal cavity and ethmoidal complex on cone-beam computed tomography. *Oral Radiology.* 2016; 33(1): 51–59, doi: [10.1007/s11282-016-0248-6](https://doi.org/10.1007/s11282-016-0248-6).
11. Dedouit F, Telmon N, Guilbeau-Frugier C, et al. Virtual anthropology and forensic identification: report of one case. *Forensic Sci Int.* 2007; 173(2-3): 182–187, doi: [10.1016/j.forsciint.2007.01.002](https://doi.org/10.1016/j.forsciint.2007.01.002), indexed in Pubmed: [17289318](https://pubmed.ncbi.nlm.nih.gov/17289318/).
12. Ekizoglu O, Hocaoglu E, Inci E, et al. Assessment of sex in a modern Turkish population using cranial anthropometric parameters. *Leg Med (Tokyo).* 2016; 21: 45–52, doi: [10.1016/j.legalmed.2016.06.001](https://doi.org/10.1016/j.legalmed.2016.06.001), indexed in Pubmed: [27497333](https://pubmed.ncbi.nlm.nih.gov/27497333/).
13. Hajjioannou J, Owens D, Whittet HB. Evaluation of anatomical variation of the crista galli using computed tomography. *Clin Anat.* 2010; 23(4): 370–373, doi: [10.1002/ca.20957](https://doi.org/10.1002/ca.20957), indexed in Pubmed: [20196125](https://pubmed.ncbi.nlm.nih.gov/20196125/).
14. Keros P. [On the practical value of differences in the level of the lamina cribrosa of the ethmoid]. *Z Laryngol Rhinol Otol.* 1962; 41: 809–813, indexed in Pubmed: [14032071](https://pubmed.ncbi.nlm.nih.gov/14032071/).
15. Kim JJ, Cho JH, Choi JW, et al. Morphologic analysis of crista galli using computed tomography. *J Rhinol.* 2012; 19: 91–95.
16. Komut E, Golpinar M. A comprehensive morphometric analysis of crista galli for sex determination with a novel morphological classification on computed tomography images. *Surg Radiol Anat.* 2021; 43(12): 1989–1998, doi: [10.1007/s00276-021-02799-2](https://doi.org/10.1007/s00276-021-02799-2), indexed in Pubmed: [34245351](https://pubmed.ncbi.nlm.nih.gov/34245351/).
17. Kranioti EF, Işcan MY, Michalodimitrakis M. Craniometric analysis of the modern Cretan population. *Forensic Sci Int.* 2008; 180(2-3): 110.e1–110.e5, doi: [10.1016/j.forsciint.2008.06.018](https://doi.org/10.1016/j.forsciint.2008.06.018), indexed in Pubmed: [18718728](https://pubmed.ncbi.nlm.nih.gov/18718728/).
18. Krogman WM, Iscan MY. *The Human Skeleton in Forensic Medicine*, Charles C. Thomas. Springfield IL 1986.
19. Manea C, Mladina R. Crista galli sinusitis – a radiological impression or a real clinical entity. *Rom J Rhinol.* 2016; 6(23): 167–171, doi: [10.1515/rjr-2016-0019](https://doi.org/10.1515/rjr-2016-0019).
20. Mladina R, Antunović R, Cingi C, et al. An anatomical study of pneumatized crista galli. *Neurosurg Rev.* 2017; 40(4): 671–678, doi: [10.1007/s10143-017-0825-0](https://doi.org/10.1007/s10143-017-0825-0), indexed in Pubmed: [28168617](https://pubmed.ncbi.nlm.nih.gov/28168617/).
21. Ogawa Y, Imaizumi K, Miyasaka S, et al. Discriminant functions for sex estimation of modern Japanese skulls. *J Forensic Leg Med.* 2013; 20(4): 234–238, doi: [10.1016/j.jflm.2012.09.023](https://doi.org/10.1016/j.jflm.2012.09.023), indexed in Pubmed: [23622466](https://pubmed.ncbi.nlm.nih.gov/23622466/).
22. Paber J, Cabato M, Villarta R, et al. Radiographic analysis of the ethmoid roof based on KEROS classification among filipinos. *Philipp J Otolaryngol Head Neck Surg.* 2008; 23(1): 15–19, doi: [10.32412/pjohns.v23i1.763](https://doi.org/10.32412/pjohns.v23i1.763).
23. Paknahad M, Shahidi S, Zarei Z. Sexual dimorphism of maxillary sinus dimensions using cone-beam computed tomography. *J Forensic Sci.* 2017; 62(2): 395–398, doi: [10.1111/1556-4029.13272](https://doi.org/10.1111/1556-4029.13272), indexed in Pubmed: [27864961](https://pubmed.ncbi.nlm.nih.gov/27864961/).
24. Poje G, Mladina R, Skitarelic N, et al. Some radiological and clinical aspects of the sinus crista galli. *Roman J Rhinol.* 2014; 13: 31–36.
25. Şahan MH, Inal M, Muluk NB, et al. Cribriform plate, crista galli, olfactory fossa and septal deviation. *Curr Med Imaging Rev.* 2019; 15(3): 319–325, doi: [10.2174/1573405614666180314150237](https://doi.org/10.2174/1573405614666180314150237), indexed in Pubmed: [31989883](https://pubmed.ncbi.nlm.nih.gov/31989883/).
26. Saini V, Srivastava R, Rai RK, et al. An osteometric study of northern Indian populations for sexual dimorphism in craniofacial region. *J Forensic Sci.* 2011; 56(3): 700–705, doi: [10.1111/j.1556-4029.2011.01707.x](https://doi.org/10.1111/j.1556-4029.2011.01707.x), indexed in Pubmed: [21361935](https://pubmed.ncbi.nlm.nih.gov/21361935/).
27. Sangvichien S, Boonkaew K, Chuncharunee A, et al. Sex determination in Thai skulls by using craniometry: multiple logistic regression analysis. *Siriraj Med J.* 2007; 59: 216–221.
28. Scarfe WC, Farman AG, Sukovic P. Clinical applications of cone-beam computed tomography in dental practice. *J Can Dent Assoc.* 2006; 72(1): 75–80, indexed in Pubmed: [16480609](https://pubmed.ncbi.nlm.nih.gov/16480609/).
29. Som PM, Park EE, Naidich TP, et al. Crista galli pneumatization is an extension of the adjacent frontal sinuses. *AJNR Am J Neuroradiol.* 2009; 30(1): 31–33, doi: [10.3174/ajnr.A1291](https://doi.org/10.3174/ajnr.A1291), indexed in Pubmed: [18768714](https://pubmed.ncbi.nlm.nih.gov/18768714/).
30. Tetiker H, Kosar M, Çullu N, et al. Pneumatization of crista galli in Pre-adult and Adult Stages. *Int J Morphol.* 2016; 34(2): 541–544, doi: [10.4067/s0717-95022016000200021](https://doi.org/10.4067/s0717-95022016000200021).
31. Thai L, Syed AZ, Palomo M, et al. revalence of pneumatization of the crista galli in dental patients. *Oral Surg Oral Med Oral Pathol Oral Radiol.* 2019; 128(4): e176–e177, doi: [10.1016/j.oooo.2019.01.064](https://doi.org/10.1016/j.oooo.2019.01.064).
32. Uçar H, Bahşi I, Orhan M, et al. The radiological evaluation of the crista galli and its clinical implications for anterior skull base surgery. *J Craniofac Surg.* 2021; 32(5): 1928–1930, doi: [10.1097/SCS.00000000000007507](https://doi.org/10.1097/SCS.00000000000007507), indexed in Pubmed: [33534307](https://pubmed.ncbi.nlm.nih.gov/33534307/).
33. Verma R, Krishan K, Rani D, et al. Estimation of sex in forensic examinations using logistic regression and likelihood ratios. *Forensic Scien Int Reports.* 2020; 2: 100118, doi: [10.1016/j.fsir.2020.100118](https://doi.org/10.1016/j.fsir.2020.100118).